Journal of Physics and Chemistry of Solids 114 (2018) 53–57

Contents lists available at ScienceDirect

Journal of Physics and Chemistry of Solids

journal homepage: www.elsevier.com/locate/jpcs

Trap distribution in $AgIn_5S_8$ single crystals: Thermoluminescence study

S. Delice [a,*], M. Isik [b], N.M. Gasanly [c,d]

[a] Department of Physics, Hitit University, 19040 Çorum, Turkey
[b] Department of Electrical and Electronics Engineering, Atilim University, 06836 Ankara, Turkey
[c] Department of Physics, Middle East Technical University, 06800 Ankara, Turkey
[d] Virtual International Scientific Research Centre, Baku State University, 1148 Baku, Azerbaijan

ARTICLE INFO

Keywords:
Chalcogenides
Defects
Luminescence

ABSTRACT

Distribution of shallow trap levels in $AgIn_5S_8$ crystals has been investigated by thermoluminescence (TL) measurements performed below room temperature (10–300 K). One broad TL peak centered at 33 K was observed as constant heating rate of 0.2 K/s was employed for measurement. The peak shape analysis showed that the TL curve could consist of several individual overlapping TL peaks or existence of quasi-continuous distributed traps. Therefore, TL experiments were repeated for different stopping temperatures (T_{stop}) between 10 and 34 K with constant heating rate of 0.2 K/s to separate the overlapping TL peaks. The E_t vs T_{stop} indicated that crystal has quasi-continuously distributed traps having activation energies increasing from 13 to 41 meV. Heating rate effect on trapped charge carriers was also investigated by carrying out the TL experiments with various heating rates between 0.2 and 0.6 K/s for better comprehension of characteristics of existed trap levels. Analyses indicated that the trap levels exhibited the properties of anomalous heating rate behavior which means the TL intensity and area under the TL peak increase with increasing heating rate.

1. Introduction

I-III-VI ternary chalcogenides have recently been studied by many researchers due to their physical and chemical properties. They are significant candidates to be used in solar cell applications as a photoabsorber because of their wide range of band gap between 0.8 and 2.0 eV [1]. They can become an important part of the industrial devices like optoelectronic, photovoltaic and photo-electrochemical devices since they exhibit good radiation stability and high absorption in active visible light [2,3]. Conversion between n- and p-type semiconductors can be achieved easily by varying the compositions in these ternary chalcogenides. These semiconductors possess considerable properties which make them potentially applicable for photoconductors, LEDs, infrared detectors, charge storage, and visible light photocatalysis [4–9]. Among these semiconductors, $AgIn_5S_8$ crystals have attracted much interest and have been studied in many areas. Their optical and electrical properties were reported in Refs. [10–13]. Since they show noticeable physical and chemical properties, they can be considered as practicable material for photovoltaic and photo-electro chemical devices [14,15].

Previously, $AgIn_5S_8$ semiconductors have been investigated by means of their optical and electrical properties. They have direct energy band gaps of 1.78 and 1.88 eV at 295 and 96 K, respectively [11]. Photoluminescence (PL) investigations have been achieved between 1.44 and 1.91 eV energy regions below room temperature (10–170 K) [16]. The detected PL spectrum, having maximum at 1.65 eV, revealed the presence of donor-acceptor pair located at $E_d = 0.06$ eV below the conduction band and at $E_a = 0.32$ eV above the valence band. Defect characterization of $AgIn_5S_8$ crystals has also been established by thermally stimulated current measurements performed in temperature region of 10–70 K with heating rate of 0.2 K/s [17]. One peak was observed in the spectrum and thermal activation energy of associated trapping level was found as 5 meV. Bucurgat et al. [18] have studied the spectral distribution of photocurrent (PC) response of $AgIn_5S_8$ crystals at various temperatures ranging from 80 to 300 K. The PC spectrum exhibited one broad peak and the band gap of the crystal was found as 1.86 eV at 140 K.

In this manuscript, characterization of defects which influence the electrical and optical efficiency of the semiconducting materials has been studied by the help of thermoluminescence (TL) measurements. TL spectra observed between 10 and 300 K have been analyzed using different methods known from the TL theory. Distribution of trapping levels has been investigated by utilizing different stopping temperatures. Activation energies of these levels have been calculated and heating rate

* Corresponding author.
E-mail address: serdardelice@hitit.edu.tr (S. Delice).

https://doi.org/10.1016/j.jpcs.2017.11.011
Received 13 September 2017; Received in revised form 5 November 2017; Accepted 9 November 2017
Available online 10 November 2017

Fig. 1. Grown $AgIn_5S_8$ single crystals.

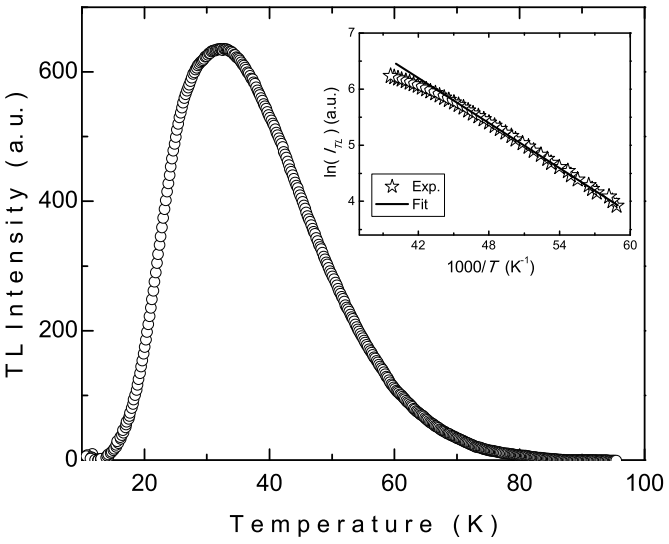

Fig. 2. Experimental TL peak of $AgIn_5S_8$ crystals detected with $\beta = 0.2$ K/s. Inset: Application of initial rise method. Stars and solid line depict the experimental data and linear fit, respectively.

dependency of TL peakhas been investigated.

2. Experimental

$AgIn_5S_8$ polycrystals were synthesized from high-purity elements (at least 99.999%) prepared in stoichiometric proportions. Single crystals of $AgIn_5S_8$ were grown by the Bridgman method in evacuated (10^{-5} Torr) silica tubes (10 mm in diameter and about 25 cm in length) with a tip at the bottom in our crystal growth laboratory. The ampoule was moved in a vertical furnace through a thermal gradient of 30 °C/cm between the temperatures 1130 and 840 °C at a rate of 1.0 mm/h. The resulting ingots presented in Fig. 1 showed good optical quality. Atomic composition of the studied sample was revealed earlier by energy dispersive spectroscopy measurements in our published paper [19]. Analyses showed that atomic composition ratios of constituent elements Ag:In:S is 7.4:37.8:54.8. Crystal structure of the sample was also reported in Ref. [19] as a result of x-ray diffraction measurements. Crystal structure of the sample was revealed as cubic unit cell with lattice parameter of $a = 1.0827$ nm. This reported crystal structure parameter is in good agreement with $a = 1.0820$ nm given in Ref. [20].

Thermoluminescence experiments were performed with a setup built in the laboratory. The measurement system was assembled around a closed cycle helium gas cryostat (Advanced Research Systems, Model CSW 202) which has capability of controlling the temperature between 10 and 300 K. Environment of the sample was kept at the intended temperature employing a temperature controller (Lakeshore Model 331). The device can control the temperature of the sample up to 300 K and can ramp the temperature linearly at a maximum rate of 1.2 K/s. In our TL experiment, the temperature of the environment was decreased to $T_0 = 10$ K and the sample was exposed to blue LED (~470 nm) for 600 s at this temperature. After an expectation time (120 s) the sample in the form of disk of diameter 8 mm and thickness 3 mm was heated up to 300 K. Thermally emitted luminescence from the sample was compiled by a light tight measurement chamber that had a photomultiplier (PM) tube (Hamamatsu R928, spectral response: 185–900 nm) and some optic elements focusing the luminescence to PM tube. These optics were attached to the optical access port of the cryostat with quartz window. The pulses from the PM tube were converted into transistor-transistor logic pulses (0–5 V) using a fast amplifier/discriminator (Hamamatsu Photon Counting Unit C3866) and were counted using the counter of a data acquisition module (National Instruments, NI 6211). All of the measurement setup were managed with a central system by improving a software written in LabView (National Instruments).

3. Results and discussion

Fig. 2 shows the TL spectrum of $AgIn_5S_8$ crystals recorded with constant heating rate of 0.2 K/s below room temperature (10–100 K). The remaining part of the spectrum (100–300 K) was not presented in the figure since it exhibited no peak after 100 K. In our experiments carried out for determination of activation energy we used the lower heating rate $\beta = 0.2$ K/s to prevent the deviation on the position of TL peak and so to obtain the correct value of activation energy. Clearly, using the higher heating rates can lead to differences between the temperature of the sample and the recorded temperature of the heater element due to some possible cases such as sample thickness and temperature gradients through the sample etc. This event is known as temperature lag effect and affects the position of the TL peaks [21–23]. Another reason of using lower heating rate is based on the fact that overlapped TL peaks have higher probability to be separated from each other. Therefore, lower heating rates give more reliable results than higher heating rates. As seen from the figure, one broad TL peak starting around 12 K and disappearing nearly at 85 K was detected from the TL emission of the studied sample. Although the observed peak points out the existence of one peak related to one single trap center at first glance, it can possess many overlapping individual peaks associated with many trapping levels or quasi-continuously distributed traps due to its broadening shape. In order to elucidate this broadening behavior of TL peak, some analyses have been taken under consideration in the present study. Inset of Fig. 2 reveals the logarithmic plot of TL intensity as a function of reciprocal of temperature. This plot is known as initial rise method [24]. According to this method, concentration of trapped charge carriers unremarkably varies with temperature at the beginning part of the ascendant tail of the TL peak. Under the light of this fact, the known TL equations giving TL intensity reduce to a simple form as $I_{TL}(T) \approx A\exp(-E_t/kT)$, which is independent of order of kinetics [24]. As understood from this relation, ln (I_{TL}) vs. $1/T$ plot presents straight line yielding a slope of $-E_t/k$ in which E_t defines the activation energy of the trap center. Inset of Fig. 2 illustrates such a plot of the observed TL peak. Activation energy of trapped charge carriers was found as 13 meV by the application of initial rise method. This value may be related to the shallowest trap level in the $AgIn_5S_8$ crystals.

Peak shape method presents an insight about understanding the

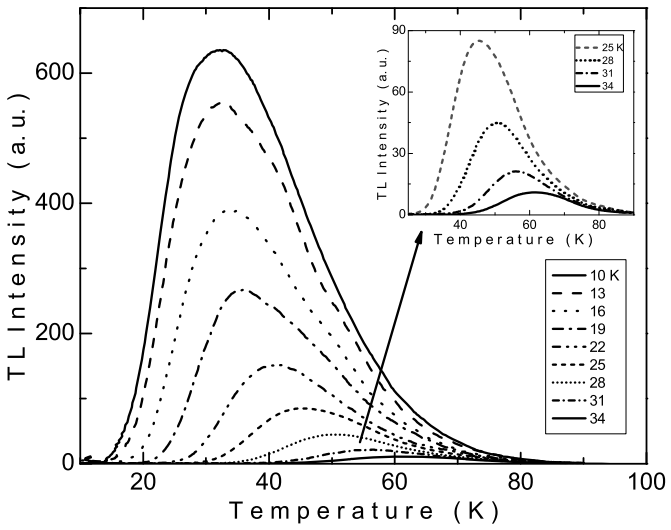

Fig. 3. Experimental TL peaks of $AgIn_5S_8$ crystals obtained with $\beta = 0.2$ K/s at different T_{stop}. Inset: Representation of TL peaks obtained with T_{stop} between 25 and 34 K.

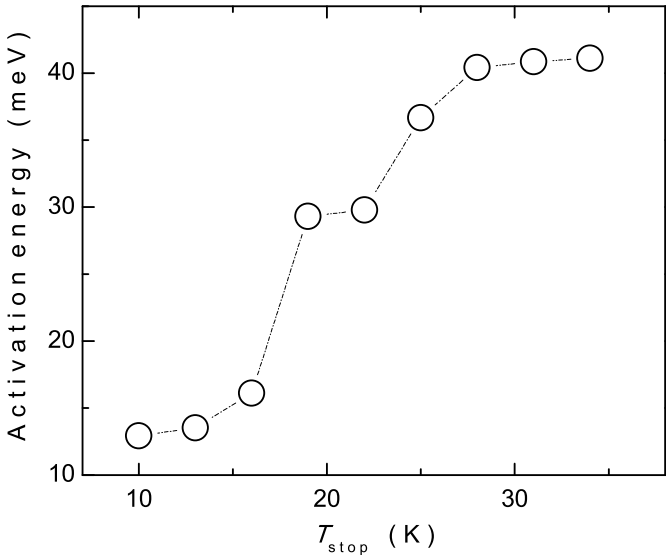

Fig. 4. E_t vs T_{stop} graph. Circles show the calculated activation energies.

behavior of the TL peaks [25]. This method is very useful since it achieves calculating the geometry factor (μ_g) of TL peak. This factor gives information about the kinetics order of TL process of trapped charge carriers. The μ_g value can be obtained by using the low (T_l) and high (T_h) temperature sides of the TL peak, which coincide with the half of the peak maximum intensity, in the following equations $\delta = T_h - T_{max}$, $w = T_h - T_l$ and $\mu_g = \delta/w$. Chen and Kirsh claim that this value must be between 0.42 and 0.52 which correspond to first- and second-order of kinetics, respectively. Implementation of this method to our observed TL curve gave the μ_g value as 0.62 that is out of the accepted values. This is an indication that the detected TL peak is not an individual peak.

Thermally cleaning procedure is the most suitable way to deplete some of the traps taking role in the existence of broad TL peak. This procedure was applied to observed TL peak for different stopping temperature (T_{stop}) sequentially. Clearly, the temperature of the studied sample was decreased to T_{stop} value and the sample was illuminated for 600 s at this temperature. Then, the sample was cooled down to 10 K. Constant heating rate of 0.2 K/s was employed to increase the temperature of the sample up to 300 K and TL peak was detected. The same processes were carried out

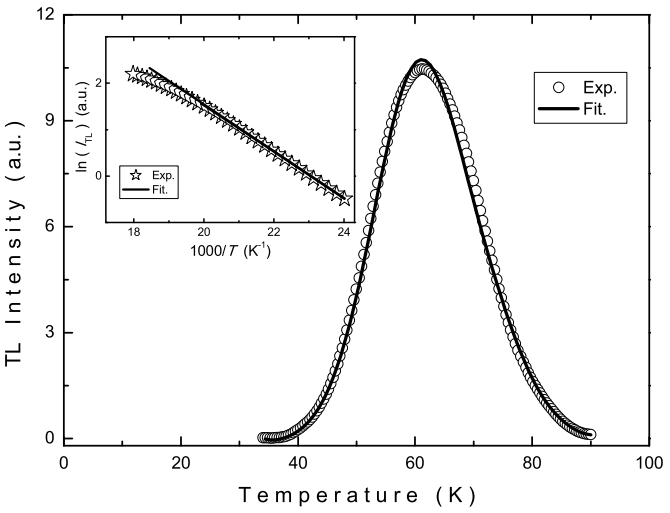

Fig. 5. Experimental TL peak of $AgIn_5S_8$ crystals obtained with $\beta = 0.2$ K/s at $T_{stop} = 34$ K. Circles and solid line represent the experimental data and curve fit, respectively. Inset: Ln (I_{TL}) vs $1000/T$ graph. Stars and solid line depict the experimental data and linear fit, respectively.

for different T_{stop} values between 10 and 34 K to obtain the successive TL peaks. Fig. 3 illustrates the TL peaks recorded for above mentioned heating rate and T_{stop} values. As can be seen from the figure, the TL intensity of the presented peaks decreases and the T_{max} value gradually shifts to higher temperatures with increasing T_{stop}. Each successive TL peak shows that the shallower levels are emptied gradually and only the charge carriers occupying the deeper levels contribute to TL peak as the higher T_{stop} is employed. The TL intensity of the peak observed for $T_{stop} = 34$ K is almost depleted as seen in the inset of Fig. 3. The behavior of T_{max}–T_{stop} dependency was investigated by McKeever [26]. In the paper it was reported that T_{max}–T_{stop} dependency has three different relations. If T_{max} increases with T_{stop} linearly as observed in our experiments, this points out the existence of quasi-continuous distribution of TL peaks. Therefore, we believe that studied crystal $AgIn_5S_8$ have quasi-continuous distributed trapping centers in the forbidden band gap. The activation energies of shallowest trap within the distributed traps were evaluated by applying the initial rise method to each successive TL peak. Fig. 4 shows the E_t vs T_{stop} graph for $AgIn_5S_8$ crystals. As seen from the figure, activation energies of distributed traps increase from 13 to 41 meV.

As we mentioned previously, the TL peak detected at $T_0 = 10$ K (see Fig. 3) had broadening shape and it was found out that the main TL peak comprised of continuously distributed traps. Normally, as the thermally cleaning procedure is realized for the bigger T_{stop} values, the concentration of trapping charge carriers in shallower trapping levels is depleted and geometry of the TL peak obtained from deeper trap levels changes. Thus, the trapping characteristics of individual trap levels can be determined. In order to better comprehend the characteristics of individual trap levels corresponding to individual TL peaks, we analyzed the whole TL peaks obtained with all experienced T_{stop} values. The peak shape method was implemented to the TL peaks and the μ_g values were calculated as given in Table 1. Here, the geometry factors calculated for the TL peaks observed between $T_{stop} = 10$ and 31 K are bigger than 0.52 that is above the threshold value. However, the μ_g value of the TL peak recorded for $T_{stop} = 34$ K was computed as nearly 0.52. This value indicated that the other shallower trap levels in distribution were completely or substantially emptied as the $T_{stop} = 34$ K was employed. Supportively, we applied the curve fitting method to this peak under the light of TL equation responsible for second order of kinetics [24]. The TL peak was successfully fitted as seen in Fig. 5. Also, ln (I_{TL}) vs $1/T$ graph was presented in the inset of Fig. 5. The activation energy values obtained from those of two methods were in good agreement with the value of 41 meV.

Table 1
Geometry factors (μ_g) of TL glow peaks of $AgIn_5S_8$ crystals obtained with different T_{stop}.

T_{stop} (K)	10	13	16	19	22	25	28	31	34
μ_g	0.62	0.62	0.68	0.65	0.60	0.61	0.57	0.56	0.52

Fig. 6 presents the TL peaks of $AgIn_5S_8$ crystals observed with various heating rates ranging from 0.2 to 0.6 K/s. As seen from the figure, the T_{max} value shifts towards higher temperatures with higher heating rates as expected. The shift of T_{max} with increase of β was explained in Ref. [27] in the study on lithium magnesium borate phosphors. For a used heating rate of β_1, phosphors spend a certain time at a temperature T_1. So, an amount of thermal release of electrons at T_1 could take place. At a higher heating rate of β_2, phosphors spend shorter time at the same temperature T_1. Consequently, there occur some decrease in the amount of thermally released electrons. A higher temperature T_2 is needed to release the same amount of electrons for heating rate β_2. This way, the TL glow curve shifts to higher temperatures for higher heating rates. Although T_{max}–β dependency obeys theoretical expectation, the TL intensity rises with increasing heating rate unlike the normal heating rate dependence. Thermal activation energy can be computed utilizing the heating rate dependency of empirical TL peaks. The following equation gives the heating rate dependence of T_{max} as known from the TL theory [24].

$$\beta = (\nu k/E_t)T_{max}^2 exp(-E_t/kT_{max}).$$

The T_{max} in the exponential term dominantly affects the position of TL peaks. Therefore, plotting ln (β) vs. $1/T_{max}$ graph yields a straight line. The slope of this plot is equal to $-E_t/k$. We applied this method to our observed TL peaks as seen in the inset of Fig. 6. The slope of the graph gave the activation energy value as 12 meV. This value is consistent with the activation energy value of the shallowest trap level (13 meV) in the crystal. This can be an indication that the T_{max} value of the first peak within distribution is nearly same with the T_{max} value of the TL peak observed for $T_0 = 10$ K.

For better comprehension of heating rate effect on TL peak, we expanded our analyses and plotted the graph giving the dependencies of peak maximum intensity, peak maximum temperature, full-widths-half-maximum (FWHM) and area (S_0) enclosed under the TL peaks (see Fig. 7). The T_{max} and FWHM values increase from 33 to 43 K and from 26 to 42 K, respectively. Also, the I_{TL} and S_0 values increase 1.3 and 2 folds, respectively. These observations are not compatible with the well-known normal heating rate behavior. Unlikely, such a behavior was explained with the phenomenon called as anomalous heating rate behavior [28–31]. This behavior can be simply elucidated as the competition between the radiative and non-radiative transitions. The number of the radiative transitions elevates while the same number of the non-radiative transitions diminishes for charge conservation [31]. The detailed discussion was reported in our previous studies [32,33]. Using the same phenomenon, the increase of the area under the TL peaks (200% enhancement), which can be ascribed to ascendancy of radiative transitions probability over that of non-radiative transitions, established the anomalous heating rate behavior.

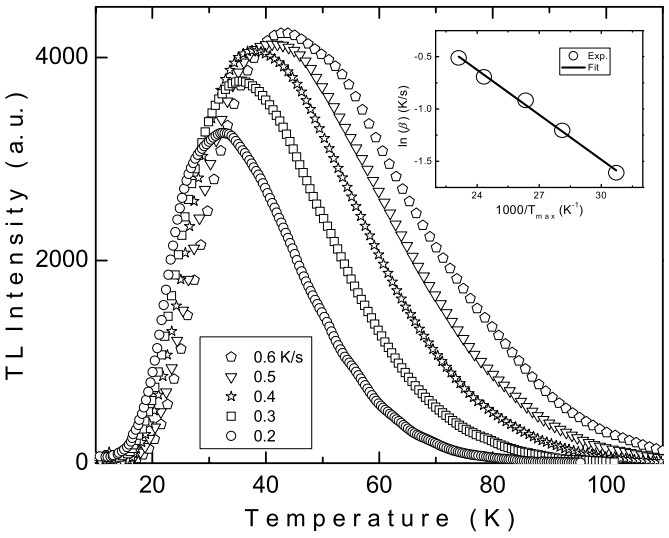

Fig. 6. Experimental TL peaks of $AgIn_5S_8$ crystals observed with various β between 0.2 and 0.6 K/s. Inset: Ln(β)–1000/T_{max} plot. Circles and solid line are experimental data and linear fit, respectively.

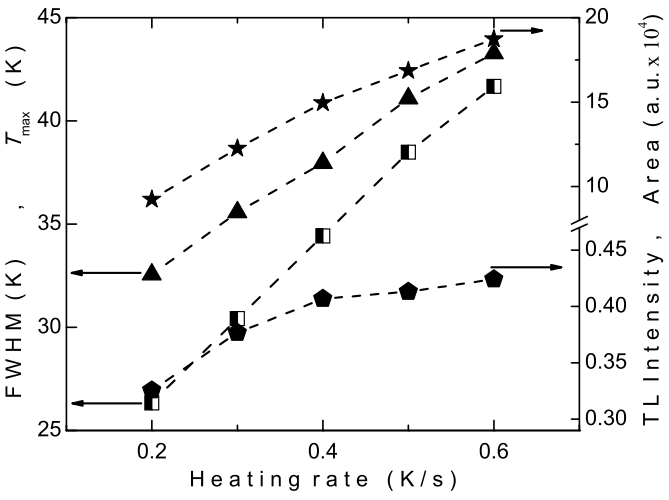

Fig. 7. The heating rate dependencies of the peak maximum temperature, the full-width-half-maximum, the TL intensity and the area (S_0) of the TL peaks.

4. Conclusion

Thermoluminescence characterization of the defect levels in $AgIn_5S_8$ crystals has been achieved by analyzing the TL peaks appearing with the application of thermally cleaning process for different T_{stop} values between 10 and 34 K. E_t–T_{stop} dependency showed that the broad TL peak observed with heating rate of 0.2 K/s consisted of superposition of continuously distributed TL peaks. Activation energies of the traps were found as increasing from 13 to 41 meV. It was thought that the TL peak observed with $T_{stop} = 34$ K had own individual TL peak. The μ_g value of 0.52 and the successful curve fit with second order TL equation indicated that the other shallowest trap levels were completely or substantially emptied and the trap level exhibited the characteristics of non-first order of kinetics which meant retrapping were not negligible. Heating rate dependency of TL peaks obtained with rates between 0.2 and 0.6 K/s was investigated. Anomalous behavior was ascribed to trap levels since the TL intensity and area under the TL peaks increased nearly 130 and 200%, respectively, which revealed the emitted luminescence raised with elevating heating rate.

References

[1] S.M. Sze, Physics of Semiconductor Devices, John Wiley & Sons, New York, 1981.
[2] M. Gannouni, I. Ben Assaker, R. Chtourou, Experimental investigation of the effect of indium content on the $CuIn_5S_8$ electrodes using electrochemical impedance spectroscopy, Mater. Res. Bull. 61 (2015) 519–527.

[3] N. Khemiri, M. Kanzari, Investigation on dispersive optical constants and electrical properties of $CuIn_5S_8$ thin films, Solid State Commun. 160 (2013) 32–36.
[4] I.V. Bodnar, Thermal expansion of $CuIn_5S_8$ single crystals and the temperature dependence of their band gap, Semiconductors 46 (2012) 602–605.
[5] D. Chen, J. Ye, Photocatalytic H-2 evolution under visible light irradiation on $AgIn_5S_8$ photocatalyst, J. Phys. Chem. Solids 68 (2007) 2317–2320.
[6] K.W. Cheng, S.C. Wang, Influences of chelating agents on the growth and photoelectrochemical response of chemical bath synthesized $AgIn_5S_8$ film electrodes, Sol. Energy Mater. Sol. Cells 93 (2009) 307–314.
[7] A.O. Pudov, J.R. Sites, M.A. Contreras, T. Nakada, H.W. Schock, CIGS J-V distortion in the absence of blue photons, Thin Solid Films 480 (2005) 273–278.
[8] H. Goto, Y. Hashimoto, K. Ito, Efficient thin film solar cell consisting of TCO/CdS/$CuInS_2$/$CuGaS_2$ structure, Thin Solid Films 451 (2004) 552–555.
[9] N.G. Dhere, Scale-up issues of CIGS thin film PV modules, Sol. Energy Mater. Sol. Cells 95 (2011) 277–280.
[10] G.E. Delgado, A.J. Mora, Structural characterization of the semiconductor chalcogenide system Ag-In-VI (VI= S, Se, Te) by X-ray powder diffraction, Chalcogenide Lett. 6 (2009) 635–639.
[11] N.S. Orlova, I.V. Bodnar, E.A. Kudritskaya, Crystal growth and properties of the $CuIn_5S_8$ and $AgIn_5S_8$ compounds, Cryst. Res. Technol. 33 (1998) 37–42.
[12] S.J. Lee, J.E. Kim, H.Y. Park, Optical absorption of Co^{2+} in $AgIn_5S_8$ and $CuIn_5S_8$ spinel crystals, Jpn. J. Appl. Phys. 42 (2003) 3337–3339.
[13] P. Yao, D. Wei, X. Zhao, S.Z. Kang, X. Li, J. Mu, Facile preparation of $AgIn_5S_8$ pompon-like microspheres with high visible light photocatalytic activity, Adv. Mater. Res. 239–242 (2011), 3302-+.
[14] I.V. Bodnar, V.F. Gremenok, V.Yu Rud, YuV. Rud, Production and investigation of $AgIn_5S_8$/(InSe, GaSe) heterojunctions, Semiconductors 33 (1999) 740–743.
[15] C.H. Lai, C.Y. Chiang, P.C. Lin, K.Y. Yang, C.C. Hua, T.C. Lee, Surface-engineered growth of $AgIn_5S_8$ crystals, ACS Appl. Mater. Interfaces 5 (2013) 3530–3540.
[16] N.M. Gasanly, A. Serpenguzel, A. Aydinli, O. Gurlu, I. Yilmaz, Donor-acceptor pair recombination in $AgIn_5S_8$ single crystals, J. Appl. Phys. 85 (1999) 3198–3201.
[17] T. Yildirim, N.M. Gasanly, Shallow trapping center parameters in as-grown $AgIn_5S_8$ crystals determined by thermally stimulated current measurements, Cryst. Res. Technol. 44 (2009) 1267–1271.
[18] M. Bucurgat, S. Ozdemir, T. Fırat, Photocurrent analysis of $AgIn_5S_8$ crystal, Bull. Mater. Sci. 39 (2016) 1521–1529.
[19] M. Isik, N. Gasanly, Ellipsometry study of optical parameters of $AgIn_5S_8$ crystals, Phys. B 478 (2015) 127–130.
[20] A. Usujima, S. Takeuchi, S. Endo, T. Irıe, Optical and electrical properties of $CuIn_5S_8$ and $AgIn_5S_8$ single crystals, Jpn. J. Appl. Phys. 20 (1981) 1505–1507.
[21] D.S. Betts, L. Couturier, A.H. Khayrat, B.J. Luff, P.D. Townsend, Temperature distribution in thermoluminescence experiments. 1.Experimental results, J. Phys. D. Appl. Phys. 26 (1993) 843–848.
[22] D.S. Betts, P.D. Townsend, Temperature distribution in thermoluminescence experiments. 2.Some calculational models, J. Phys. D. Appl. Phys. 26 (1993) 849.
[23] T.M. Piters, A.J.J. Bos, Effects of nonideal heat-transfer on the glow curve in thermoluminescence experiments, J. Phys. D. Appl. Phys. 27 (1994) 1747.
[24] R. Chen, S.W.S. McKeever, Theory of Thermoluminescence and Related Phenomena, World Scientific, Singapore, 1997.
[25] R. Chen, Y. Kirsh, Analysis of Thermally Stimulated Processes, Pergamon Press, Oxford, 1981.
[26] S.W.S. McKeever, On the analysis of complex thermoluminescence glow-curves: resolution into individual peaks, Phys. Stat. Sol. A 62 (1980) 331–340.
[27] S.R. Anishia, M.T. Jose, O. Annalakshmi, V. Ramasamy, Thermoluminescence properties of rare earth doped lithium magnesium borate phosphors, J. Luminescence 131 (2011) 2492–2498.
[28] A.J.J. Bos, N.R.J. Poltoon, J. Wallinga, A. Bessiere, P. Dorenbos, Energy levels in YPO_4:Ce^{3+},Sm^{3+} studied by thermally and optically stimulated luminescence, Radiat. Meas. 45 (2010) 343–346.
[29] R. Chen, J.L. Lawless, V. Pagonis, Two-stage thermal stimulation of thermoluminescence, Radiat. Meas. 47 (2012) 809–813.
[30] A. Mandowski, A.J.J. Bos, Explanation of anomalous heating rate dependence of thermoluminescence in YPO_4:Ce^{3+},Sm^{3+} based on the semi-localized transition (SLT) model, Radiat. Meas. 46 (2011) 1376–1379.
[31] V. Pagonis, L. Blohm, M. Brengle, G. Mayonado, P. Woglam, Anomalous heating rate effect in thermoluminescence intensity using a simplified semi-localized transition (SLT) model, Radiat. Meas. 51–52 (2013) 40–47.
[32] S. Delice, E. Bulur, N.M. Gasanly, Anomalous heating rate dependence of thermoluminescence in Tl_2GaInS_4 single crystals, J. Mater. Sci. 49 (2014) 8294–8300.
[33] S. Delice, E. Bulur, N.M. Gasanly, Thermoluminescence in gallium sulfide crystals: an unusual heating rate dependence, Phill. Mag. 95 (2015) 998–1006.